Origin and palaeoenvironmental significance of C_{25} and C_{27} *n*-alk-1-enes in a 25,000-year lake-sedimentary record from equatorial East Africa

L.G.J. van Bree[a,b*], W.I.C. Rijpstra[a], C. Cocquyt[c, d], N.A. Al-Dhabi[e], D. Verschuren[d], J.S. Sinninghe Damsté[a,b], J.W. de Leeuw[a, e]

[a] NIOZ Royal Netherlands Institute for Sea Research, Department of Marine Organic Biogeochemistry, P.O. Box 59, 1790 AB Den Burg, The Netherlands.

[b] Utrecht University, Faculty of Geosciences, Department of Earth Sciences, P.O. Box 80.021, 3508 TA Utrecht, The Netherlands

[c] National Botanic Garden of Belgium, Domein van Bouchout, B-1860 Meise, Belgium

[d] Ghent University, Limnology Unit, K.L. Ledeganckstraat 35, B-9000 Gent, Belgium

[e] Department of Botany and Microbiology, Addiriyah Chair for Environmental Studies, College of Science, King Saud University, P.O. Box 2455, Riyadh 11451, Saudi Arabia

*Corresponding author. Utrecht University, Faculty of Geosciences, Department of Earth Sciences, P.O. Box 80.021, 3508 TA Utrecht, The Netherlands. L.G.J.vanBree@uu.nl. +31 30 253 52 32

Abstract

We studied the distribution of long-chain alkenes (*n*-C_{23} to *n*-C_{31}) in well-dated sediments from Lake Challa, a deep crater lake near Mt. Kilimanjaro in equatorial East Africa, to reveal signatures of palaeo-environmental and palaeo-climatic changes affecting the production of these compounds during the last 25 kyr. The apolar fractions of organic sediment extracts dated to the last 16 kyr showed an unusual dominance of δ^{13}C-depleted *n*-$C_{25:1}$ and *n*-$C_{27:1}$ alk-1-enes. These alkenes were not detected in soil and litter from near the shoreline and from the inner rim of the crater, pointing to an autochthonous, aquatic source. Analysis of suspended particulate matter indicated that the *n*-alk-1-enes are produced in the well-oxygenated upper 30 m of the water column, indicating a phytoplanktonic origin. Sedimenting particles collected monthly from December 2006 to November 2007 showed increased fluxes of *n*-alk-1-enes following the

locally prominent short rain season in November-December. Green algae and/or cyanobacteria were identified as candidate sources of these alkenes. Production of the *n*-$C_{25:1}$ and *n*-$C_{27:1}$ alkenes in Lake Challa was much reduced during the Last Glacial Maximum and early late-glacial period, suggesting a temperature or CO_2 effect on habitat suitability. We explored the potential of *n*-alk-1-ene accumulation rates, and of a derived Alkene Index [*n*-$C_{27:1}$]/([*n*-$C_{25:1}$]+[*n*-$C_{27:1}$]), to record longer-term climatic changes. The Alkene Index record of Lake Challa over the past 25 kyr shows clear periodicity with a dominant frequency of ~2.3 kyr, potentially indicative of monsoon variability directly or indirectly forced by variation in solar radiation.

1. Introduction

Lake sediments are excellent archives of past environmental and climate changes. Organic biomarkers of lake sediments have contributed substantially to climate history reconstructions of Africa (e.g. Tierney et al., 2008; Verschuren et al., 2009; Sinninghe Damsté et al., 2011). The occurrence of long-chain *n*-alkenes (*n*-C_{23} to *n*-C_{31}) in various types of lacustrine sediments has frequently been reported (e.g. Jaffé et al., 1996; Zhang et al., 2004, 2011;Theissen et al., 2005; de Mesmay et al., 2007), but even though these potential biomarkers sometimes dominate the apolar fraction of organic sediment extracts, their origin and fate remains ambiguous and are sometimes not even addressed. One major reason for this apparently modest interest is that sedimentary *n*-alkenes can have multiple natural sources. Short-chain *n*-alkenes (<*n*-C_{22}) can derive from cyanobacteria, microalgae, macroalgae and zooplankton, while long-chain *n*-alkenes (>*n*-C_{22}) are traditionally thought to be derived from either higher plant waxes (Eglinton and Hamilton, 1967) or microalgae (e.g. Gelpi et al., 1968, 1970; Cardoso et al., 1983, Jaffé et al., 1996; Volkman et al., 1998). Because of these different possible origins, the distribution of *n*-alkenes in lacustrine sediment records often leads to disparate interpretations. In some studies they are argued to derive from allochthonous sources such as higher plants, including marginal reeds, ferns and peat (Giger et al., 1980; Cardoso et al., 1983; Cranwell et al., 1987; Duan and Ma, 2001). In other studies the compounds are attributed to an autochthonous (aquatic) source, such as algae in general (Jaffé et al., 1996; Zhang et al., 2004; Xu and Jaffé, 2009), cyanobacteria (Gelpi et al., 1970), or specific algal species such as the green alga *Botryococcus*

braunii race A (Theissen et al., 2005). Some studies interpret the *n*-alkenes as resulting from a mixture of both microalgae and higher plant input (e.g. Zhang et al., 2011).

In this paper we describe the stratigraphic distribution of two specific *n*-alkenes in the anoxic bottom sediments of Lake Challa, a permanently stratified crater lake on the border of Tanzania and Kenya. The origin and potential palaeoenvironmental significance of these two long-chain *n*-alkenes are discussed based on ecological and sedimentary data.

2. Materials and methods

2.1 Study area: Lake Challa

Lake Challa (3°19'S, 37°42'E) is a crater lake of approximately 4.5 km^2 surface area with a maximum depth of 92 m in 2005. This tropical freshwater lake is located ~880 m above sea level, on the lower south-east slope of Mt. Kilimanjaro in equatorial East Africa (Fig. 1). Rainfall seasonality is mainly determined by the twice-annual passing of the Inter-Tropical Convergence Zone (ITCZ). This results in relatively moderate "long rains" from March to May, and heavy "short rains" from October to December. The local precipitation/evaporation balance is negative, and balanced by subsurface inflow of groundwater derived from rain falling higher up on Mt. Kilimanjaro. Temporary discharge from a creek breaching the northwestern crater rim can occur during heavy rains. Allochthonous organic matter in Lake Challa sediments consists of wind-blown particles from the surrounding savanna landscape, supplemented by soil erosion and litter input from the inner crater rim. Seasonal deep mixing of the water column extends down to 40-60 m between June and September, when air and surface water temperature are lowest, while daily wind-driven mixing is limited to 15-20 m year-round. A constant temperature of 22.2°C and complete anoxia at greater depths indicate that the lower water column is permanently stratified, or at most mixes with a decadal or lower frequency (Wolff et al., 2011; Sinninghe Damsté et al., 2012).

Rainfall in the Lake Challa area is mainly influenced by insolation-driven monsoon intensity. Today, both the El Nino-Southern Oscillation (ENSO) and the Indian Ocean dipole or Zonal Mode (IOZM) can have a strong non-linear impact on rainfall amount and intensity during the "short rains" in October-December (Black et al., 2003; Mölg et al., 2006; Tierney et al., 2011). Lake Challa is located east of the Congo Air Boundary (CAB) throughout the year, which

minimizes the influence of northern high-latitude climate signatures propagated to low latitudes by the Atlantic Meridional Overturning Circulation (AMOC; Verschuren et al., 2009). Lake Challa is, therefore, an ideal location to study long-term changes in insolation-driven monsoon intensity and the associated precipitation.

2.2 Study material

We studied a 21.65-m long composite sequence of mostly finely laminated organic-rich muds, based on several cores from the center of Lake Challa (Fig. 1) obtained in 2003 and 2005 as reported by Verschuren et al. (2009). After excision of five turbidites, it yielded a 20.82-m long sequence of continuous offshore lacustrine sedimentation covering ca. 25,000 years (25 kyr). The age-depth model is based on a smoothed spline through INTCAL04-calibrated AMS ^{14}C ages of 164 bulk organic carbon samples, corrected for a variable old-carbon age offset of between 200 and 450 yr (Blaauw et al., 2011). For the present analysis of organic biomarkers, sediment samples with 4-cm thickness, each comprising about 50 years, were extracted at ~200 yr intervals throughout the last 25 kyr. In total 146 sediment samples were analyzed both quantitatively and qualitatively, of which 105 represent the Holocene (the last 11.7 kyr). The exceptionally precise age model (Blaauw et al., 2011) allowed the calculation of sedimentary biomarker fluxes. An additional 24 samples were analyzed only qualitatively, for determination of the alkene ratio. The stable carbon isotopic composition of *n*-alkenes was analyzed in 12 samples.

A sediment-trap was installed in November 2006 at 35 m water depth (Fig. 1). Samples for biomarker analysis were retrieved at ca. 4-week intervals up to December 2007, as described by Sinninghe Damsté et al. (2009). For the purpose of this study, a preserved subsample of the filtered sediment-trap material was used for phytoplankton analyses. Algal and cyanobacterial remains were brought back in suspension with distilled water, and filters were carefully checked for any remaining material. The algal suspension was then diluted to a known volume and studied following the Uthermöhl (1931) method using sedimentation chambers of 10 ml and an inverted Olympus CX41 microscope.

Suspended particulate matter (SPM) was sampled on 10-11 September 2006 at 13 depth intervals along a vertical profile in the center of the lake (Fig. 1). Water volumes of 4 to 9 L were

retrieved from every 5 m between 0 and 30 m, and every 10 m between 30 and 90 m depth. The water was filtered through GFF filters and stored frozen until processing. As in Sinninghe Damsté et al. (2009), data from the deepest SPM sample (90 m) was excluded since a contribution of resuspended uppermost bottom sediments was evident. As the SPM samples were collected over a 2-day period, these data provide only a snapshot of the expected large changes in primary productivity, linked to the seasonal cycle of Lake Challa.

Eight soil samples were collected in the catchment area of Lake Challa in 2005 (Fig. 1) as described by Sinninghe Damsté et al. (2009). Sampling of litter was performed in September 2012 (Fig. 1). Three near-shore litter samples represent plant and fruit remains, decomposing flat leaves and leaf stalks of the hydrophilous sedge *Cyperus involucratus*; two litter samples from about halfway up the crater rim consist of leaf and twig remains and small non-determinable particles.

2.3 Lipid analysis

The freeze-dried and powdered sediments were extracted with a Dionex™ Accelerated Solvent Extractor (ASE) using a dichloromethane (DCM)/methanol (9:1, v/v) mixture at high temperature (100 °C) and pressure (7.6 x 10^6 Pa). The total organic extracts were separated over a column with activated Al_2O_3 into an apolar and a polar fraction using hexane/DCM (9:1, v/v) and DCM/MeOH (1:1, v/v) as eluents, respectively. The apolar fraction was analyzed by gas chromatography (GC) and GC-mass spectrometry (MS) after adding a known amount of internal standard (pristane). Quantification of compounds was performed by peak area integration of the chromatograms. The double-bond position of the mono-unsaturated alkenes was determined on the basis of mass spectra of their dimethyl disulfide derivatives as described by Nichols et al. (1986). Fluxes (in mg m^{-2} yr^{-1}) of the quantified apolar compounds were calculated taking into account their concentration, the measured water content and the dry weight of sediment samples.

SPM and sediment-trap samples were extracted as described before (Sinninghe Damsté et al., 2009). The apolar fractions of the sediment extracts were obtained by column chromatography over Al_2O_3 by elution with hexane/DCM (9:1, v/v). Pristane was added as internal standard before analysis by GC and GC/MS. Fluxes of *n*-alkenes (in mg m^{-2} yr^{-1}) were calculated for

sediment-trap samples, taking into account the dry sample weight, days of collection and funnel size of the sediment-trap device.

Leaf, stem and fruit remains present in some litter samples were cut into small pieces. All litter and soil samples were ultrasonically extracted with DCM/MeOH (2:1, v/v). The extracts were evaporated to dryness, methylated with diazomethane in ether and separated over a column filled with activated Al_2O_3 into an apolar and polar fraction, as described above. The apolar fractions were analyzed by GC and GC-MS.

GC was performed using a Hewlett-Packard (HP6890) instrument equipped with an on-column injector and a flame ionization detector. A fused silica capillary column (25 m x 0.32 mm) coated with CP Sil-5 CB (film thickness 0.12 µm) was used with helium as carrier gas. The samples were injected at 70 °C and the oven temperature was programmed to 130 °C at 20 °C/min and then at 4 °C/min to 320 °C, at which it was held for 20 min. GC-MS was performed on a Finnigan Trace DSQ mass spectrometer operated at 70 eV with a mass range of *m/z* 40 to 800 and a cycle time of 1.7 s. The gas chromatograph was equipped with a fused silica capillary column as described above for GC. The carrier gas was helium, and the same oven temperature program as for GC was used. For the SPM samples, single ion monitoring (SIM) was conducted on the $M^{+\bullet}$ ions (m/z 350.0-351.0 and 378.0-379.0) of the C_{25} and C_{27} *n*-alk-1-enes to further support their identification, as their concentrations were low.

The apolar fractions of 12 selected sediments younger than 17 kyr BP and one sediment-trap sample were separated into a saturated and an unsaturated hydrocarbon fraction using a small column with Ag+-impregnated silica and hexane and ethyl acetate as eluents, respectively. Both saturated and unsaturated hydrocarbon fractions were subjected to compound-specific $\delta^{13}C$ analysis using an Agilent 6800 GC coupled to a ThermoFisher Delta V isotope-ratio monitoring mass spectrometer. Carbon isotope values were measured against calibrated external reference gas and performance of the instrument was monitored by daily injections of a mixture of a C_{20} and a C_{24} perdeuterated *n*-alkane with known isotopic compositions. The $\delta^{13}C$ values are reported in the standard delta notation against the Vienna Pee Dee Belemnite (VPDB) standard. All samples were run at least in duplicate, with an average standard deviation of 0.5‰ for the C_{25} *n*-alkene and 0.4‰ for the C_{27} *n*-alkene.

Spectral analysis of the proxy data set was undertaken using AnalySeries software (Paillard et al., 1996). The Alkene Index record was detrended using a polynomial function, interpolated to a constant ~200-yr interval and analyzed with the Blackman-Tukey method. Frequencies around ~2.3 kyr were filtered from the record (Gaussian filter centered at 0.00044, bandwidth 0.0001) excluding superimposed low and high frequencies. REDFIT analysis was conducted with PAST software (Hammer et al., 2001) for significance estimation.

3. Results

3.1 Sediments

Fig. 2 shows typical distribution patterns of apolar lipids in Lake Challa sediments. Most sediments contain *n*-alkanes, *n*-alkenes, phytadienes, hopenes and des-A-triterpenoids (with lupane, oleanane, ursane and arborane skeletons). In sediments younger than 16 kyr BP, two unusually dominant components are the *n*-$C_{25:1}$ and *n*-$C_{27:1}$ alkenes. DMDS adduction indicated a terminal position of the double bond in these *n*-$C_{25:1}$ and *n*-$C_{27:1}$ alkenes. The *n*-$C_{23:1}$ alkene was found only at some depth intervals and in low concentrations, and low or trace amounts of *n*-$C_{26:1}$ and *n*-$C_{29:1}$ alkenes were encountered occasionally in the younger sediments. A few sediment intervals also contained traces of an *n*-C_{27} alkadiene.

The accumulation rate of *n*-alkenes is highest in the younger, uppermost sediments (Fig. 3). The accumulation rate of *n*-$C_{25:1}$ alkene mostly exceeds 1 mg m^{-2} yr^{-1} in sediments younger than 3.9 kyr BP, with a pronounced maximum (5 mg m^{-2} yr^{-1}) in sediments dated to ~600 year BP. The accumulation of *n*-$C_{27:1}$ alkene is high between 8.8 and 7.2 kyr BP and after 3.5 kyr BP, with a pronounced peak of 4.5 mg m^{-2} yr^{-1} at 3.5-3.2 kyr BP. Accumulation rates of both *n*-$C_{25:1}$ and *n*-$C_{27:1}$ alkenes are low (<0.14 mg m^{-2} yr^{-1}) before 16 kyr BP, with slightly higher values at 23.1-22.5 and 19.3 kyr BP. The mean long-term trend in both *n*-alkenes is similar, with average accumulation rates of 0.1 mg m^{-2} yr^{-1} in the Last Glacial Maximum (LGM) and early late glacial periods (25 to ~16 kyr BP), and 1.8 mg m^{-2} yr^{-1} during the Holocene. The here defined Alkene Index, defined as [*n*-$C_{27:1}$]/([*n*-$C_{25:1}$]+[*n*-$C_{27:1}$]), varies from 0.36 to 0.92 over the past 25 kyr (Fig. 3D), with higher (>0.75) values mostly restricted to sediments older than 6 kyr BP.

3.2 Settling particles

The apolar lipid fractions of the extracts of settling particles contain mainly *n*-alkanes (*n*-C_{23} to *n*-C_{35}), *n*-alkenes (*n*-C_{23} to *n*-C_{31}), hopenes and some des-A-triterpenoids (with ursane and lupane skeletons). The fluxes and distribution patterns of *n*-$C_{25:1}$ and *n*-$C_{27:1}$ alkenes varied through the year (Fig. 4). Fluxes of *n*-$C_{25:1}$ and *n*-$C_{27:1}$ alkenes (Fig. 4A-B) were both highest during the first month of deployment (December 2006) and lower thereafter, resembling the total mass flux of depositing material and organic carbon (cf. Sinninghe Damsté et al., 2009). The annual flux of *n*-alk-1-enes into the sediment-trap is comparable but slightly lower (with *n*-$C_{25:1}$ and *n*-$C_{27:1}$ alkene accumulations of 1.1 and 1.3 mg m^{-2} yr^{-1}, respectively) than the average Holocene *n*-alk-1-ene accumulation rate in the sediment (1.2 and 1.8 mg m^{-2} yr^{-1}, respectively). The Alkene Index varied between 0.5 and 0.9 with highest values in January and August-November 2007 (Fig. 4D), i.e. generally coinciding with the dry seasons. The annual pattern in the flux of *n*-alkenes is roughly similar to the combined monthly flux of small *Cosmarium* spp. (green algae) in the same sediment-trap samples (Fig. 4E).

3.3 Suspended particulate matter

The *n*-$C_{25:1}$ and *n*-$C_{27:1}$ alkenes were detected in SPM from the upper water column down to 40 m depth, i.e., within the oxic part of the water column, in concentrations of up to 8.1 and 21 ng L^{-1}, respectively (Fig. 5). In SPM from the lower water column these alkenes were not detected, or present in much lower concentrations only.

3.4 Soils and litter

The apolar lipid fractions of soil and litter from the Challa crater catchment contained mainly *n*-alkanes (*n*-C_{25} to *n*-C_{33}), squalene and plant-derived triterpenoids. Long-chain *n*-$C_{25:1}$ and *n*-$C_{27:1}$ alkenes were not detected. In one litter sample containing plant fruit remains, *n*-alkenes (*n*-C_{23} to *n*-C_{35}) were present, but these compounds did not contain a terminal double bond.

3.5 Stable carbon isotopic composition

The stable carbon isotopic composition of the *n*-alkenes from Lake Challa sediments varied substantially, from -44‰ to -37‰ within the last 17 kyr (Fig. 3E; Table 1). Typically, the *n*-$C_{25:1}$ alkene is slightly less depleted than the *n*-$C_{27:1}$ alkene, with average values of -39.4±0.5‰ and -40.8±0.5‰, respectively. The *n*-alkenes are also isotopically depleted compared to the

corresponding *n*-alkanes, the latter ranging from -40 to -25‰ (Table 1). The higher *n*-alkanes are less depleted and show an increasingly less negative average value than the average isotopic signatures of *n*-C_{25} (-36‰), *n*-C_{27} (-35‰) and *n*-C_{29} (-31‰) alkanes. The $\delta^{13}C$ values of *n*-$C_{25:1}$ and *n*-$C_{27:1}$ alkenes in the sediment-trap sample of December 2006 are -34‰ and -39‰, respectively, which is in the range of measurements of the corresponding sedimentary *n*-alkenes but notably somewhat more positive, especially in the case of the *n*-$C_{25:1}$ alkene.

4. Discussion

4.1 Origin of the *n*-$C_{25:1}$ and *n*-$C_{27:1}$ alkenes

The origin of *n*-$C_{25:1}$ and *n*-$C_{27:1}$ alkenes in lacustrine sediments is not self-evident, as *n*-alkenes are biosynthesized by widely different (groups of) organisms. Diagenetic transformations of functionalized compounds such as alcohols are a possible source of *n*-alkenes in sediments. However, dehydration of the dominant even-carbon numbered alcohols found in Lake Challa sediments would generate even carbon-numbered *n*-alkenes instead of the dominant *n*-$C_{25:1}$ and *n*-$C_{27:1}$ alkenes. Decarboxylation of even-chain fatty acids could yield odd-chain hydrocarbons, but in Lake Challa this diagenetic origin is unlikely, since only two odd-chain *n*-alk-1-enes are encountered in high relative abundances in the study material.

A variety of higher plants are known to produce *n*-alk-1-enes. Cardoso et al. (1983) identified the fern *Dryopteris dilatata* and erosion from peat deposits as most likely sources of sedimentary *n*-alkenes in Rostherne Lake (England). In that study, the fern and peat contained homologous series of *n*-alkenes (*n*-C_{18} to *n*-C_{32}) with a dominance of *n*-$C_{29:1}$ and *n*-$C_{31:1}$. This typical higher-plant distribution is not seen in the sediments of Lake Challa. The complete absence of *n*-alk-1-enes in all soil and litter samples from Challa crater further suggests an origin different than land plants. Aeolian input with *n*-$C_{25:1}$ and *n*-$C_{27:1}$ alkenes derived from regional terrestrial vegetation is not likely either. To the best of our knowledge, *n*-alkenes have not been reported as constituents of aeolian transported spores, pollen or wax components. Aquatic macrophytes can also be excluded as a source due to their absence along the very steep-sloping and rocky shoreline of Lake Challa (Fig. 1). Even the substantial lake-level lowering which occurred during the early late-glacial period (Moernaut et al. 2010) is not likely to have created more favorable conditions for development of aquatic macrophytes (Sinninghe Damsté et al., 2011).

Insects are known to produce *n*-alkenes, and although Lake Challa sediments contain microfossil remains of chironomid larvae (Eggermont and Verschuren, 2004) an insect origin of *n*-alkenes in Lake Challa is unlikely. Insects show a characteristically broad range of (branched) *n*-alkenes with high carbon numbers (*n*-C_{24} to *n*-C_{45}; Blomquist and Jackson, 1979), including some *n*-$C_{25:1}$ and *n*-$C_{27:1}$ alkenes (Oudejans and Zandee, 1973; Chikaraishi et al., 2012), but also many others. In microbial mats (Boudou et al., 1986a; 1986b) predominantly *n*-C_{29} and *n*-C_{31} *n*-alkenes of insect origin were present. Furthermore, to the best of our knowledge, Eubacteria do not produce *n*-$C_{25:1}$ and *n*-$C_{27:1}$ alkenes. The *n*-alkenes produced by insects and in microbial mats do not match with the specific alkene distribution encountered in Lake Challa sediments.

Significant concentrations of the *n*-alkenes were detected in SPM of the upper water-column and in the sediment-trap, indicating autochthonous biogenic production of the *n*-$C_{25:1}$ and *n*-$C_{27:1}$ alkenes by organisms living in the (most often) well-oxygenated upper 40 m of the water column. This origin is supported by the significant $\delta^{13}C$ offset between the *n*-alkenes and corresponding *n*-alkanes derived from terrestrial vegetation. The $\delta^{13}C$ values of the *n*-alkenes are up to 7‰ (*n*-$C_{25:1}$) and 9‰ (*n*-$C_{27:1}$) more negative than their corresponding *n*-alkanes (Table 1). The more negative $\delta^{13}C$ values of the *n*-alkenes compared to those derived from land plants (higher *n*-alkanes and also land-derived triterpenes, latter data not shown) are consistent with the expected carbon-isotopic depletion of algal sources in Lake Challa.

Some freshwater species of both cyanobacteria and microalgae are known to synthesize *n*-alkenes. Cyanobacteria can contain a wide range of *n*-alkenes (e.g. Gelpi et al., 1968; 1970; Cardoso et al., 1983): species include *Oscillatoria* sp., which contains *n*-$C_{21:1}$ to *n*-$C_{23:1}$ alkenes (Matsumoto et al., 1990) and *Anacystis montana,* common in eutrophic lakes, is reported as a source of *n*-C_{19} to *n*-C_{29} alkenes (Gelpi et al., 1968). Gelpi et al. (1968; 1970) detected predominantly *n*-$C_{25:1}$ and *n*-$C_{27:1}$ alkenes in *A. montana*, but this finding is disputed by Murray and Thomson (1977) since their axenic *A. montana* cultures contained no long-chain *n*-alkenes at all. Similarly, non-axenic cultures of *Microcystis aeruginosa* contained *n*-alk-1-enes, while they were not detected in axenic cultures (Cardoso et al., 1983). Paoletti et al. (1976) found only small or trace amounts of *n*-$C_{20:1}$, *n*-$C_{23:1}$ and *n*-$C_{27:1}$ *n*-alkenes in four non-axenic cultures (*Spirulina platensis*, *Spirulina* sp., *Calothrix* sp. and *Nostoc commune*). It is questionable whether cyanobacteria produce *n*-alkenes. The *n*-alkene distribution so far observed in single

cyanobacterial species does not fit the *n*-alkene distribution found in Lake Challa, and the often trace amounts of *n*-alkenes cannot explain the dominance of *n*-alkenes in the apolar lipid fractions of Lake Challa sediments.

Some microalgae produce *n*-alk-1-enes. The green alga *B. braunii* race A contains *n*-C_{23} to *n*-C_{33} alkenes (e.g. Gelpi et al., 1970) and the eustigmatophyte *Nannochloropsis* spp. contains *n*-C_{15} to *n*-C_{31} alkenes (Gelin et al., 1997). In both *Nannochloropsis* spp. and *B. braunii* race A, the *n*-alk-1-enes are accompanied by significant amounts of alkadienes, trienes or *n*-$C_{23:1}$ and *n*-$C_{29:1}$ alkenes. In the sediments of Lake Challa, only minor amounts of *n*-$C_{23:1}$ and traces of *n*-$C_{29:1}$ alkenes and one *n*-$C_{27:2}$ alkadiene were detected, but no other alkadienes or trienes. Traces of the *n*-$C_{23:1}$ alkene are present in the SPM from surface waters, and a larger range of *n*-alk-1-enes from *n*-C_{21} up to *n*-C_{31}, albeit in small quantities, are present in settling particles. Since no significant amounts of alkadienes or alkatrienes are encountered either in the water column or sediments of Lake Challa, it is unlikely that species like *Nannochloropsis* spp. and *B. braunii* contribute substantially to the *n*-alk-1-enes in Lake Challa. Non-axenic cultures of the green algae *Ulothrix gigas, Uronema terrestre* and *Selenastrum gracile* contained small or trace amounts of *n*-C_{20}, *n*-C_{23} and *n*-C_{27} alkenes (Paoletti et al., 1976). The green alga *Scenedesmus quadricauda* is reported to contain a variable *n*-alkene mixture, with predominantly *n*-C_{27} alkene (Gelpi et al., 1970), *n*-$C_{21:1}$, *n*-$C_{23:1}$ and *n*-$C_{25:1}$ alkenes (Cranwell et al., 1990) or with minor amounts of *n*-$C_{20:1}$, *n*-$C_{23:1}$ and *n*-$C_{27:1}$ alkenes (Paoletti et al., 1976). This latter study identified minor amounts of *n*-$C_{23:1}$ and *n*-$C_{27:1}$ alkenes in *Chlorella* sp., while *Chlorella emersonii*, a terrestrial green alga from Europe, is known to contain both *n*-$C_{25:1}$ and *n*-$C_{27:1}$ alkenes (Afi et al., 1996). Strikingly, *Chlorella vulgaris* produced predominantly *n*-$C_{25:1}$ and *n*-$C_{27:1}$ alkenes when grown under heterotrophic conditions, whereas no *n*-alkenes were detected under phototrophic conditions (Patterson, 1967). In contrast, Afi et al. (1996) reported the absence of *n*-$C_{25:1}$ and *n*-$C_{27:1}$ alkenes in axenic phototrophic incubation studies of *C. vulgaris*, and the heterotrophically grown *C. vulgaris* culture of Řezanka et al. (1982) also did not yield the *n*-$C_{25:1}$ and *n*-$C_{27:1}$ dominated alkene distribution of Patterson (1967).

Relatively modest correlation between the $\delta^{13}C$ values of *n*-$C_{25:1}$ and *n*-$C_{27:1}$ alkenes (Fig. 6) suggests that the *n*-alkenes probably originate from two or more source organisms with varying relative abundances through time, since carbon-isotope fractionation during synthesis of the two

n-alk-1-enes within a single organism should be similar at any one time. The compounds also have a similar trend but distinctively different depth profiles (Fig. 3A, B). Although the *n*-$C_{25:1}$ and *n*-$C_{27:1}$ alkenes are closely related in structure and hence a single source organism seems likely, the $\delta^{13}C$ values and depth profiles suggest multiple source organisms.

Multiple species of green algae (including *Chlorella* sp. and *Cosmarium* spp.) were recovered by us in monthly sediment-trap samples from Lake Challa. The alkene distributions in Lake Challa sediments seem to be consistent with those reported in the literature for the green algae *Chlorella emersonii*, *C. vulgaris* and *Scenedesmus quadricauda*. Of all organisms that were microscopically identified, the pattern of *Cosmarium* spp. cells settling in the sediment-trap (Fig. 4E) is most similar to that of the *n*-alkenes extracted from the bulk sediment-trap samples. The accumulation rates of *Cosmarium* spp. and *n*-alkenes are by no means identical, but show the most similar distribution of all phytoplankton. On the basis of this data, and supported by the literature, we surmise that this group of green algae potentially synthesizes the *n*-$C_{25:1}$ and *n*-$C_{27:1}$ alkenes. Although our current hypothesis is that green algae are responsible for the synthesis of *n*-alk-1-enes in Lake Challa, more (culturing) research is needed to test this. Variation in the Alkene Index through time (Fig. 3D) could then possibly be explained by different (groups of) green algae -and possibly other algae- producing the bulk of the *n*-$C_{25:1}$ and *n*-$C_{27:1}$ alkenes at different times in the past, and/or indicate periodic adaptation of one producer group to changes in their abiotic environment. Selective degradation of individual *n*-alk-1-enes is a hypothetical possibility but chemically unlikely and not supported by the sedimentary record, since the Alkene Index does not show a single sustained trend with time.

The distribution of *n*-alk-1-enes in SPM from the water column in Lake Challa is comparable to the *n*-alkene distribution in SPM of Lake Valencia in Venezuela, a larger (~350 km^2), hyper-eutrophic tropical lake situated at 400 m above sea level, but like Lake Challa with anoxic bottom waters during (most of) the year (Jaffé and Hausmann, 1995; Jaffé et al., 1996). The concentrations of *n*-$C_{25:1}$ and *n*-$C_{27:1}$ alkenes in Lake Valencia were highest within the oxygenated part of the water column (Jaffé et al., 1996). Also the sedimentary record of Lake Valencia similarly includes relatively high concentrations of *n*-$C_{25:1}$ and *n*-$C_{27:1}$ alkenes. The origin of the *n*-alk-1-enes in Lake Valencia has not been discussed in previous studies, but Lake Challa SPM and sediment do display a comparable distribution including an origin in the

oxygenated water column. The *n*-$C_{25:1}$ and *n*-$C_{27:1}$ alkenes could, therefore, possibly be used more generally as a biomarker for the unknown source microalgae.

4.2 *n*-Alkenes and hydrology

The highly variable accumulation rate of *n*-$C_{25:1}$ and *n*-$C_{27:1}$ alkenes in Lake Challa over the past 25 kyr must reflect changes in the abundance of the organism(s) producing them, and/or changes in the amount of *n*-alkenes they biosynthesize depending on ambient environmental conditions. The most prominent feature of the Challa *n*-alkene record is their near-absence prior to 16 kyr BP (Fig. 3A, C). Their fairly abrupt appearance at that time corresponds with the post-glacial onset of a strengthened southeasterly monsoon across equatorial East Africa (Gasse et al., 2008), and thus a longer or more intense principal rain season (Verschuren et al., 2009). However, since both the periods before and after 16 kyr BP include episodes of high rainfall and episodes of drought (Fig. 7), climate-driven changes in the hydrological balance of Lake Challa are unlikely the primary cause of the long-term trend in *n*-alkene production. The principal change in environmental conditions which occurred around that time is the postglacial transition from a slightly cooler (3-4 °C) glacial climate under reduced atmospheric CO_2 concentrations to the interglacial (and present-day) warm tropical climate of this equatorial region. The TEX_{86}-inferred record of temperature change from Lake Challa (Sinninghe Damsté et al., 2012) indicates that regional warming was gradual and occurred mostly between 19 and 14 kyr BP, consistent with the timing reported elsewhere in East Africa (Powers et al., 2005; Tierney et al., 2008). The low glacial atmospheric CO_2 concentration (and thus possibly higher surface-water pH) may also have influenced the composition of the phytoplankton community at Lake Challa. We surmise that either directly or indirectly, by 16 kyr BP the increased temperature and CO_2 must have created a more optimal habitat for the local *n*-alkene producing organisms. During the Holocene period (the last 11.7 kyr), temperature variation in the tropics is generally considered to have been limited to 1-2 °C (at least at low or modest surface elevations), although actual data for inter-tropical Africa remain notably scarce (e.g., Nicholson et al., 2013) and evidence for more significant Holocene temperature anomalies have occasionally been reported (Rietti-Shati et al., 1998; Berke et al., 2012). In any case it seems unlikely that temperature change has been the main driver of the highly variable rates of *n*-alkene accumulation in Lake Challa since 16 kyr BP. In contrast, as indicated by both the seismic-reflection stratigraphy of past lake-level

changes and the organic biomarker BIT index of rainfall intensity (Fig. 7), the hydrological balance of Lake Challa has varied strongly during this period. However, notwithstanding their sizable implied magnitude, these lake-level changes do not appear to have fundamentally altered the lake's mixing regime and internal nutrient cycling. This conclusion was inferred earlier from the uninterrupted deposition of finely laminated sediments (Wolff et al., 2011), implying persistence of an anoxic deep-water column; in this study it is suggested by the relative constancy of *n*-alkene $\delta^{13}C$ depletion during the Holocene (Fig. 3E).

As indicated by the year-long sediment-trap record (Fig. 4) the settling flux of *n*-alkenes in Lake Challa is positively correlated with the amount of monthly rainfall during 2006-2007. Some caution is advised about the significance of this correlation, given that seasonal rainfall patterns in the Lake Challa area can be quite variable from year to year. The catchment area of Lake Challa is small and there is limited surface inflow by direct runoff due to the steep crater wall. Nutrients in the surface waters are mainly replenished by deep water-column mixing in the dry southern hemisphere winter months of June to August, and known to stimulate diatom blooms in Lake Challa (Barker et al. 2011; Wolff et al., 2011). Selective growth of the alkene-producing algae during the ensuing "short" rain season may occur because most diatoms are disadvantaged by the developing water-column stratification. The alkene-producing algae may also benefit from a temporarily increased influx of land-derived debris during heavy rainfall. Incidental episodes of murky waters have been reported, turning Lake Challa brown. In extreme cases one might even consider heterotrophic growth of some algae during such episodes. As indicated above, certain *Chlorella* species can produce high amounts of the *n*-$C_{25:1}$ and *n*-$C_{27:1}$ alkenes during heterotrophic growth (Patterson, 1967).

Based on currently available data we conclude that accumulation of *n*-$C_{25:1}$ and *n*-$C_{27:1}$ alkenes in Lake Challa sediments reflects autochthonous production by non-diatom microalgae, and mainly during the short period of heavy rains in November-December. This connection with the seasonal pattern of precipitation may be employed as a tentative key to interpret the longer-term variation in *n*-$C_{25:1}$ and *n*-$C_{27:1}$ alkene production observed in the sedimentary record.

Variations in *n*-alk-1-ene accumulation through time (Fig. 7A) do not show a clear, unambiguous correspondence with any of the existing palaeohydrological proxy records for Lake Challa (Fig. 7C, E). At some times low *n*-alkene accumulation corresponds with episodes of relative

drought as inferred from the BIT index and seismic record, e.g., during the Younger Dryas (YD), and high accumulation with inferred wet periods such as the wet late-Holocene conditions. At other times the high *n*-alkene accumulation corresponds with episodes of inferred drought (e.g., mid- and late-Holocene). The alkene accumulation rate thus cannot be used directly as a precipitation proxy.

The Alkene Index, on the other hand, displays broad visual correspondence with the long-term hydrogen-isotope record of leaf-wax alkanes (δD_{wax}; Tierney et al., 2011) and has some features in common with the BIT index and seismic records (Fig. 7B, E). Tierney et al. (2011) suggested that the δD_{wax} records a mixture of δD in local precipitation during the two rain seasons, and thus sedimentary δD_{wax} is firstly influenced by the intensity of East African monsoon circulation, and secondly by the seasonal distribution of annual rainfall. Most lake lowstands recorded in the seismic-reflection data of the past ca. 13 kyr (Verschuren et al., 2009; Moernaut et al., 2010) are accompanied by a decrease in the Alkene Index (Fig. 7E). The long lowstand U3 dated to between 20.5 and 14.5 kyr BP is a notable exception, possibly due to very low accumulation of *n*-alk-1-enes during that period. Features shared by the alkene and BIT index records (Figs. 7B and 7D) occur in the periods 25 to 22 kyr BP, around the YD and in the last 5.5 kyr. The BIT index is used as a proxy for monsoon rainfall intensity (Verschuren et al., 2009; Barker et al., 2011), although the direct mechanistic link remains only partly unresolved (Sinninghe Damsté et al., 2009; 2012). In conclusion, the relation between the Alkene Index and other hydrological proxies is not unambiguous, but shows interesting features nonetheless.

4.3 Cyclicity in the Alkene Index

The 25-kyr Alkene Index record from Lake Challa (Fig. 7B) displays a well-developed cyclic pattern. Since the Lake Challa sediment sequence is well-dated, sampled at high resolution and deposited through time in a stable and year-round anoxic bottom-water environment, it has the appropriate integrity to discern cyclicity in climate proxies on sub-Milankovitch time-scales. Spectral analysis (Fig. 8A) reveals a main frequency of ~2.3 kyr ($p=0.0062$). Frequencies around ~2.3 kyr were filtered from the record (Gaussian filter centered at 0.00044, bandwidth 0.0001) excluding low and high frequencies superimposed on the ~2.3 kyr cycle (Fig. 8B). The filtered cyclicity pattern (Fig. 8B) describes the predominant variability of the Alkene Index, with high

amplitude between 14 and 4 kyr BP and considerably lower amplitude between 20-15 kyr BP and during the last 3 kyr.

Similar periodicities are found in hydrological proxy records within the broader East African region. For example in the diatom-based $\delta^{18}O$ record from Lake Malawi (Barker et al., 2007), the foraminiferal record of upwelling in the Arabian Sea (Gupta et al., 2003) and the Qunf cave (Oman) speleothem $\delta^{18}O$ record (Fleitmann et al., 2007). The latter is interpreted to reflect the amount of Indian summer monsoon precipitation. The long-term variability in the Alkene Index may indeed reflect some aspect of Lake Challa paleohydrology.

Frequencies of ~2.1 to ~2.4 kyr have been reported previously in diverse climate proxy records with a worldwide distribution. They are for example identified in $\delta^{18}O$ of Greenland ice cores and Asian speleothems (~2.0-3.0 kyr: Wang et al., 2008), in dust records in peat deposits (~2.2 kyr: McGowan et al., 2010), in sediment texture in marine settings (~2.8 kyr, attributed to a 2.2 kyr cycle: Nederbragt and Thurow, 2005), in tropical sea surface temperature variability based on alkenones (~2.3 kyr: Rimbu et al., 2004) and in primary productivity of foraminifera (~2.2 kyr: Naidu and Malmgren, 1995), coccolithophores (~2.4 kyr: de Garidel-Thoron et al., 2001) and diatoms (~2.1 kyr: Hausmann et al., 2006). In these studies, the ~2.3 kyr cyclicity has been attributed either to changes in oceanic circulation and upwelling as primary drivers (e.g., Naidu and Malmgren, 1995), influenced in turn by solar activity variation such as the Hallstattzeit solar cycle (~2.1 to ~2.4 kyr; e.g., Damon and Jirikowic, 1992), or the coupling between solar irradiation and oceanic processes (e.g., de Garidel-Thoron et al., 2001). Recently it was proposed that the Hallstattzeit solar cycle may have directly influenced Holocene monsoon variability (southeast Australia: McGowan et al., 2010; Holocene East Asian monsoon: Liu et al., 2012). A dominant periodicity similar to that of the Lake Challa Alkene Index record also occurs in ^{14}C and ^{10}Be records from tree rings (~2.4 kyr: Vasiliev and Dergachev, 2002; ~2.3 kyr: Mordvinov and Kramynin, 2010). Reconstructed changes in total solar irradiance (ΔTSI) based on ^{10}Be in polar ice cores (Steinhilber et al., 2009) displays clear periodicities of ~2.3 and ~1.0 kyr. The filtered Alkene Index record is mostly in phase with the filtered ΔTSI record. Generally speaking, in periods of higher total solar irradiance relatively more *n*-$C_{27:1}$ alkene was produced in the Lake Challa water column. Considering the marked cyclicity in the Lake Challa Alkene Index record, we suggest that the population of microalgae involved in *n*-alk-1-ene

production in Lake Challa have been influenced by solar irradiation variability, which in turn can be mediated by the (sun-driven) variation in Indian Ocean monsoon strength and wind patterns.

5. Conclusion

Long-chain *n*-alkenes preserved in the Lake Challa sediment record are dominated by *n*-$C_{25:1}$ and *n*-$C_{27:1}$ alkenes. These compounds are predominantly produced in the oxic upper water column, probably by (mixotrophic) green algae, following the heavy "short rains" in November to December. Production of *n*-$C_{25:1}$ and *n*-$C_{27:1}$ alkenes in Lake Challa was much reduced during the LGM and early late-glacial period, suggesting a temperature or CO_2 effect on habitat suitability. Given the positive correlation with precipitation over the annual cycle, we explored the potential of individual *n*-alk-1-ene accumulation rates, and of a derived Alkene Index, to record longer-term hydrological changes in Lake Challa. The Alkene Index record of the past 25 kyr shows clear periodicity with a dominant frequency of ~2.3 kyr, indicative of monsoon variability directly or indirectly forced by solar radiation.

Acknowledgements

We like to thank the editor and one anonymous reviewer for valuable comments that have improved the manuscript. The fieldwork for this study was carried out with permission of the Permanent Secretary of the Ministry of Education, Science and Technology of Kenya under research permit 13/001/11C to D.V. We thank C.M. Oluseno for the sediment-trap sampling, C. Wolff for TOC measurements on settling particles, J. Moernaut for the bathymetric map, A. Mets, M. Verweij and J. Ossebaar for technical assistance, and M.L. Goudeau and L. Lourens for helpful discussions on spectral analysis. This work was performed in preparation of the International Continental Scientific Drilling Programme (ICDP) DeepCHALLA project, on research materials made available through the ESF Euroclimate project CHALLACEA which is financially supported by Grants from the Dutch Organization for Scientific Research (NWO) and FWO Vlaanderen (Belgium) to J.S.S.D. and D.V., respectively.

References

Afi L., Metzger P., Largeau C., Connan J., Berkaloff C. and Rousseau B. (1996) Bacterial degradation of green microalgae: incubation of *Chlorella emersonii* and *Chlorella*

vulgaris with *Pseudomonas oleovorans* and *Flavobacterium aquatile*. *Org. Geochem.* **25**, 117-130.

Barker P. A., Leng M. J., Gasse G. and Huang Y. (2007) Century-to-millennial scale climatic variability in Lake Malawi revealed by isotope records. *Earth Planet. Sci. Lett.* **261**, 93-103.

Barker P. A., Hurrell E. R., Leng M. J., Wolff C., Cocquyt C., Sloane H. J. and Verschuren, D. (2011) Seasonality in equatorial climate over the past 25 k.y. revealed by oxygen isotope records from Mount Kilimanjaro. *Geology* **39**, 1111-1114.

Blaauw M., van Geel B., Kristen I., Plessen B., Lyaruu A., Engstrom D. R., van der Plicht J. and Verschuren D. (2011) High-resolution ^{14}C dating of a 25,000-year lake-sediment record from equatorial East Africa. *Quat. Sci. Rev.* **30**, 3043-3059.

Black E., Slingo J. and Sperber K. R. (2003) An observational study of the relationship between excessively strong short rains in coastal East Africa and Indian Ocean SST. *Mon. Weather Rev.* **131**, 74-94.

Berke M. A., Johnson T. C., Werne J. P., Schouten S. and Sinninghe Damsté J. S. (2012) A mid-Holocene thermal maximum at the end of the African Humid Period. *Earth Planet. Sci. Lett.* **351-352**, 95-104.

Blomquist G. J. and Jackson L. L. (1979) Chemistry and biochemistry of insect waxes. *Prog. Lipid Res.* **17**, 319-345.

Boudou J. P., Trichet J., Robinson N. and Brassell S.C. (1986a) Lipid composition of a recent Polynesian microbial mat sequence. *Org. Geochem.* **10**, 705-709.

Boudou J. P., Trichet J., Robinson N. and Brassell S.C. (1986b) Profile of aliphatic hydrocarbons in a recent Polynesian microbial mat. *Int. J. Environ. Anal. Chem*. **26**, 137-155.

Cardoso J. N., Gaskell S. J., Quirk M. M. and Eglinton G. (1983) Hydrocarbon and fatty acid distributions in Rostherne lake sediment (England). *Chem. Geol*. **38**, 107-128.

Chikaraishi Y., Kaneko M. and Ohkouchi N. (2012) Stable hydrogen and carbon isotopic compositions of long-chain (C_{21}-C_{33}) *n*-alkanes and *n*-alkenes in insects. *Geochim. Cosmochim. Acta* **95**, 53-62.

Cranwell P. A., Eglinton G. and Robinson N. (1987) Lipids of aquatic organisms as potential contributors to lacustrine sediments II. *Org. Geochem.* **11**, 513-527.

Cranwell P. A., Jaworski G. H. M. and Bickley H. M. (1990) Hydrocarbons, sterols, esters and fatty acids in six freshwater chlorophytes. *Phytochemistry* **29**, 145-151.

Damon P. E. and Jirikowic J. L. (1992) The sun as a low-frequency harmonic oscillator. *Radiocarbon* **34**, 199-205.

de Garidel-Thoron T., Beaufort L., Linsley B. K. and Dannenmann S. (2001) Millenial-scale dynamics of the East Asian winter monsoon during the last 200,000 years. *Paleoceanography* **16**, 491-502.

de Mesmay R., Grossi V., Williamson D., Kajula S. and Derenne S. (2007) Novel mono-, di- and tri-unsaturated very long chain (C_{37}-C_{43}) *n*-alkenes in alkenone-free lacustrine sediments (Lake Masoko, Tanzania). *Org. Geochem.* **38**, 323-333.

Duan Y. and Ma L. (2001) Lipid geochemistry in a sediment core from Ruoergai Marsh deposit (Eastern Qinghai-Tibet plateau, China). *Org. Geochem.* **32**, 1429-1442.

Eggermont H. and Verschuren D. (2004) Sub-fossil Chironomidae from East Africa. 1. Tanypodinae and Orthocladiinae. *J. Paleolimnol*. **32**, 383-412.

Eglinton G. and Hamilton R. J. (1967) Leaf epicuticular waxes. *Science* **156**, 1322-1335.

Fleitmann D., Burns S. J., Mangini A., Mudelsee M., Kramers J., Villa I., Neff U., Al-Subary A. A., Buettner A., Hippler D. and Matter A. (2007) Holocene ITCZ and Indian monsoon dynamics recorded in stalagmites from Oman and Yemen (Socotra). *Quat. Sci. Rev*. **26**, 170-188.

Gasse F., Charlié F., Vincens A., Williams M. A. J. and Williamson D. (2008) Climatic patterns in equatorial and southern Africa from 30,000 to 10,000 years ago reconstructed from terrestrial and near-shore proxy data. *Quat. Sci. Rev*. **27**, 2316–2340.

Gelin F., Boogers I., Noordeloos A. M., Sinninghe Damsté J. S., Riegman R., de Leeuw J. W. (1997) Resistant biomacromolecules in marine microalgae of the classes Eustigmatophyceae and Chlorophyceae: Geochemical implications. *Org. Geochem.* **26**, 659-675.

Gelpi E., Oró J., Schneider H. J. and Bennett E. O. (1968) Olefins of high molecular weight in two microscopic algae. *Science* **161**, 700-702.

Gelpi E., Schneider H. J., Mann J. and Oró J. (1970) Hydrocarbons of geochemical significance in microscopic algae. *Phytochemistry* **9**, 603-612.

Giger W., Schaffner C. and Wakeham S. G. (1980) Aliphatic and olefinic hydrocarbons in recent sediments of Greifensee, Switzerland. *Geochim. Cosmochim. Acta* **44**, 119-129.

Gupta A. K., Anderson D. M. and Overpeck J. T. (2003) Abrupt changes in the Asian southwest monsoon during the Holocene and their links to the North Atlantic Ocean. *Nature* **421**, 354-357.

Hammer Ø, Harper D. A. T., Ryan P. D. (2001) PAST: Paleontological statistics software package for education and data analysis. *Palaeontol. Electron.* **4**.

Hausmann S., Pienitz R., St-Onge G., Larocque I. and Richard P. J. H. (2006) Lake circulation influenced by solar activity? *Geol. Soc. Am. Abst. with Programs* **38**, 264.

Jaffé R. and Hausmann K. B. (1995) Origin and early diagenesis of arborinone/isoarborinol in sediments of a highly productive freshwater lake. *Org. Geochem.* **22**, 231-235.

Jaffé R., Cabrera A., Najje N. and Carvajal-Chitty H. (1996) Organic biogeochemistry of a hypereutrophic tropical, freshwater lake – Part 1: particle associated and dissolved lipids. *Org. Geochem.* **25**, 227-240.

Liu H. Y., Lin Z. S., Qi X. Z., Li Y. X., Yu M. T., Yang H. and Shen J. (2012) Possible link between Holocene East Asian monsoon and solar activity obtained from the EMD method. *Nonlinear Proc. Geoph.* **19**, 421-430.

Matsumoto G. I., Akiyama M., Watanuki K. and Torii T. (1990) Unusual distributions of long-chain *n*-alkanes and *n*-alkenes in Antarctic soil. *Org. Geochem.* **15**, 403-412.

McGowan H. A., Marx S. K., Soderholm J. and Denholm J. (2010) Evidence of solar and tropical-ocean forcing of hydroclimate cycles in southeastern Australia for the past 6500 years. *Geophys. Res. Lett.* **37**.

Moernaut J., Verschuren D., Charlet F., Kristen I., Fagot M. and De Batist M. (2010) The seismic-stratigraphic record of lake-level fluctuations in Lake Challa: Hydrological stability and change in equatorial East Africa over the last 140 kyr. *Earth Planet. Sci. Lett.* **290**, 214-223.

Mölg T., Renold M., Vuille M., Cullen N. J., Stocker T. F. and Kaser G. (2006) Indian Ocean zonal mode activity in a multicentury integration of a coupled AOGCM consistent with climate proxy data. *Geophys. Res. Lett.* **33**.

Mordvinov A. V. and Kramynin A. P. (2010) Long-term changes in sunspot activity, occurrences of grand minima, and their future tendencies. *Sol. Phys.* **264**, 269-278.

Murray J. and Thomson A. (1977) Hydrocarbon production in *Anacystis montana* and *Botryococcus braunii*. *Phytochemistry* **16**, 465-468.

Naidu P. D. and Malmgren B.A. (1995) A 2,200 years periodicity in the Asian monsoon system. *Geophys. Res. Lett.* **22**, 2361-2364.

Nederbragt A. J. and Thurow J. (2005) Geographic coherence of millennial-scale climate cycles during the Holocene. *Palaeogeogr. Palaeoclimatol. Palaeoecol.* **221**, 313-324.

Nichols P. D., Guckert J. B. and White D. C. (1986) Determination of monounsaturated fatty acid double-bond position and geometry for microbial monocultures and complex consortia by capillary GC-MS of their dimethyl disulphide adducts. *J. Microbiol. Methods* **5**, 49–55.

Nicholson S. E., Nash D. J., Chase B. M., Grab S. W., Shanahan T. M., Verschuren D., Asrat A., Lézine A. M. and Umer M. (2013) Temperature variability over Africa during the last 2000 years. *The Holocene* **23**, 1085-1094.

Oudejans R. C. H. M. and Zandee D. I. (1973) The biosynthesis of the hydrocarbons in males and females of the milipede *Graphidostreptus tumuliporus*. *J. Insect Physiol*. **19**, 2245-2253.

Paillard D., Labeyrie L. and Yiou P. (1996) Macintosh program performs time-series analysis. *Eos, Trans. Amer. Geophys. Union* **77**, 379–379.

Paoletti C., Pushparaj B., Florenzano G., Capella P. and Lercker G. (1976) Unsaponifiable matter of green and blue-green algal lipids as a factor of biochemical differentiation of their biomasses: I. Total unsaponifiable and hydrocarbon fraction. *Lipids* **11**, 258-265.

Patterson G. W. (1967) The effect of culture conditions on the hydrocarbon content of *Chlorella vulgaris*. *J. Phycol*. **3**, 22-23.

Powers L. A., Johnson T. C., Werne J. P., Castañeda I. S., Hopmans E. C., Sinninghe Damsté J. S. and Schouten S. (2005) Large temperature variability in the southern African tropics since the Last Glacial Maximum. *Geophys. Res. Lett.* **32**.

Řezanka T., Zahradník J. and Podojil M. (1982) Hydrocarbons in green and blue-green algae. *Folia Microbiol*. **27**, 450-454.

Riettie-Shati M., Shemesh A. and Karlen W. (1998) A 3000-year climatic record from biogenic silica oxygen isotopes in an equatorial high-altitude lake. *Science* **281**, 980-982.

Rimbu N., Lohmann G., Lorenz S. J., Kim J. H. and Schneider R. R. (2004) Holocene climate variability as derived from alkenone sea surface temperature and coupled ocean-atmosphere model experiments. *Climate Dyn.* **23**, 215-227.

Sinninghe Damsté J. S., Ossebaar J., Abbas B., Schouten S. and Verschuren D. (2009) Fluxes and distribution of tetraether lipids in an equatorial African lake: Constraints on the application of the TEX_{86} palaeothermometer and BIT index in lacustrine settings. *Geochim. Cosmochim. Acta* **73**, 4232-4249.

Sinninghe Damsté J. S., Verschuren D., Ossebaar J., Blokker J., van Houten R., van der Meer M. T. J., Plessen B. and Schouten S. (2011) A 25,000-year record of climate-induced changes in lowland vegetation of eastern equatorial Africa revealed by the stable carbon-isotopic composition of fossil plant leaf waxes. *Earth Planet. Sci. Lett.* **302**, 236-246.

Sinninghe Damsté J. S., Ossebaar J., Schouten S. and Verschuren D. (2012) Distribution of tetraether lipids in the 25-ka sedimentary record of Lake Challa: Extracting reliable TEX_{86} and MBT/CBT palaeotemperatures from an equatorial African lake. *Quat. Sci. Rev*. **50**, 43-54.

Steinhilber F., Beer J. and Fröhlich C. (2009) Total solar irradiance during the Holocene. *Geophys. Res. Lett.* **36**.

Tierney J. E., Russell J. M., Huang Y.; Sinninghe Damsté J. S., Hopmans E. C. and Cohen A. S. (2008) Northern Hemisphere controls on tropical Southeast African climate during the past 60,000 years. *Science* **322**, 252-255.

Tierney J. E., Russell J. M., Sinninghe Damsté J. S., Huang Y. and Verschuren D. (2011) Late Quaternary behavior of the East African monsoon and the importance of the Congo Air Boundary. *Quat. Sci. Rev*. **30**, 798-807.

Theissen K. M., Zinniker D. A., Moldowan J. M., Dunbar R. B. and Rowe H. D. (2005) Pronounced occurrence of long-chain alkenones and dinosterol in a 25,000-year lipid molecular fossil record from Lake Titicaca, South America. *Geochim. Cosmochim. Acta* **69**, 623-636.

Uthermöhl H. (1931) Neue Wege in der quantitativen Erfassung des Planktons. *Verh. Int. Ver. Theor. Angew. Limnol*. **5**, 567-596.

Vasiliev S. S. and Dergachev V. A. (2002) The ~2400-year cycle in atmospheric radiocarbon concentration: bispectrum of ^{14}C data over the last 8000 years. *Ann. Geophys*. **20**, 115-120.

Verschuren D., Sinninghe Damsté J. S., Moernaut J., Kristen I., Blaauw M., Fagot M. and Haug G. H. (2009) Half-precessional dynamics of monsoon rainfall near the East African Equator. *Nature* **462**, 637-641.

Volkman J. K., Barrett S. M., Blackburn S. I., Mansour M. P., Sikes E. L. and Gelin F. (1998) Microalgal biomarkers: a review of recent research developments. *Org. Geochem.* **29**, 1163-1179.

Wang Y., Cheng H., Edwards R. L., Kong X., Shao X., Chen S., Wu J., Jiang X., Wang X. and An Z. (2008) Millennial- and orbital-scale changes in the East Asian monsoon over the past 224,000 years. *Nature* **451**, 1090-1093.

Wolff C., Haug G. H., Timmermann A., Sinninghe Damsté J. S., Brauer A., Sigman D. M., Cane M. A. and Verschuren D. (2011) Reduced interannual rainfall variability in East Africa during the Last Ice Age. *Science* **333**, 743-747.

Xu Y. and Jaffé R. (2009) Geochemical record of anthropogenic impacts on Lake Valencia, Venezuela. *Appl. Geochem*. **24**, 411-418.

Zhang Z., Zhao M., Yang X., Wang S., Jiang X., Oldfield F. and Eglinton G. (2004) A hydrocarbon biomarker record for the last 40 kyr of plant input to Lake Heqing, southwestern China. *Org. Geochem.* **35**, 595-613.

Zhang Z., Metzger P. and Sachs J. P. (2011) Co-occurrence of long chain diols, keto-ols, hydroxy acids in keto acids in recent sediments of Lake El Junco, Galápagos Islands. *Org. Geochem.* **42**, 823-837.

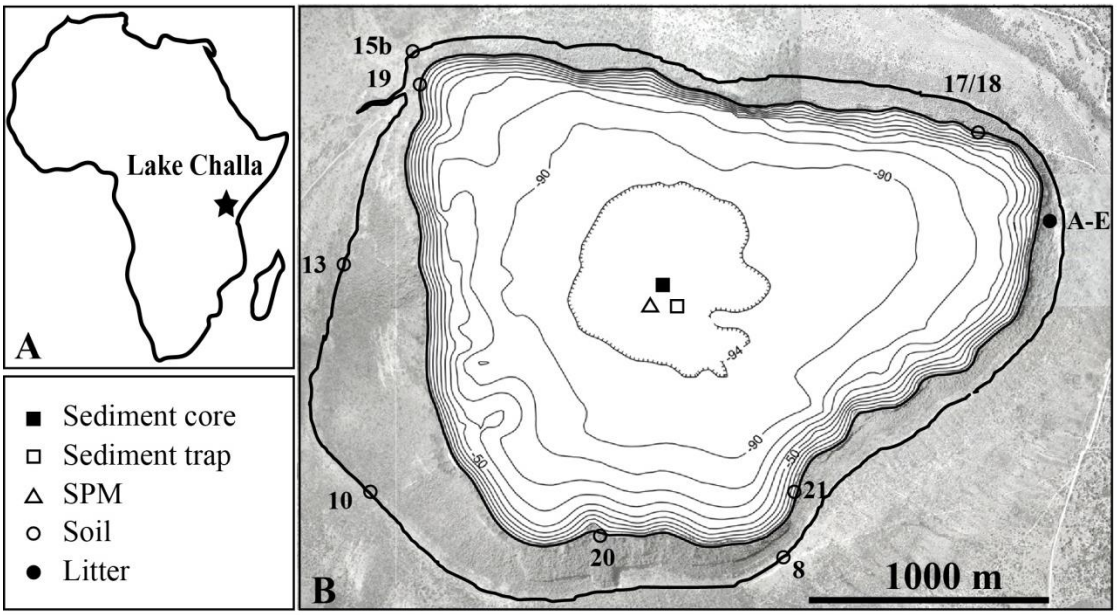

Figure 1: Lake Challa (3°19'S, 37°42'E) on the border of Kenya/Tanzania in equatorial East Africa [A] with bathymetry at 10-m intervals and sampling locations of the suspended particulate matter (SPM) profile (△), the sediment-trap (□) and the long sediment core (■), as well as catchment soil (○) and litter (●) samples [B]. The inner bold line represents the lake shore at the time of coring in 2005, whereas the outer bold line indicates the crater rim, which forms the edge of the catchment area. Modified after Moernaut et al. (2010).

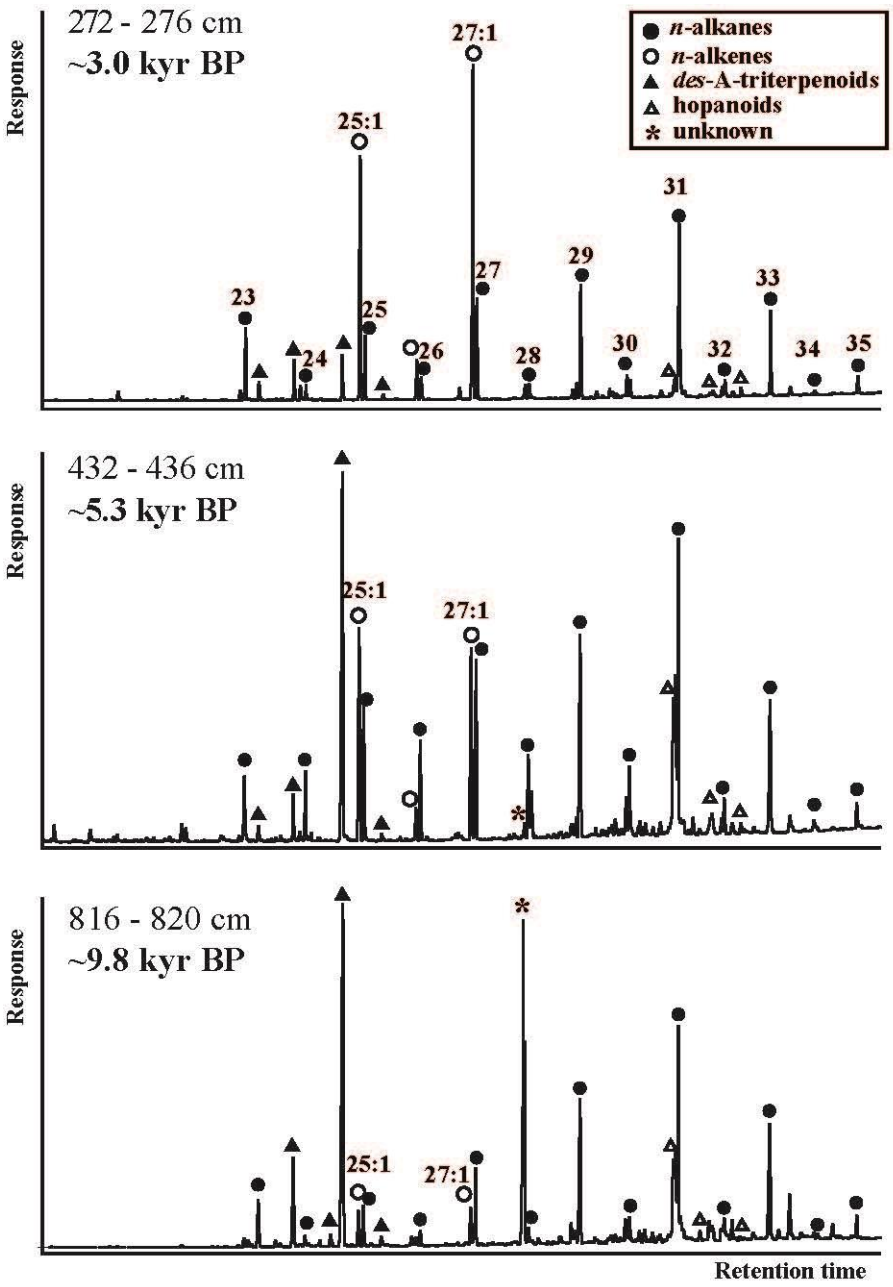

Figure 2: GC-FID traces of the apolar fractions of organic extracts from three sediment samples dated to the Holocene (age and composite profile depth indicated) attributable to *n*-alkanes (●), *n*-alk-1-enes (⭘), des-A-triterpenoid hydrocarbons (▲), hopanoids (△) and an unknown compound (*).

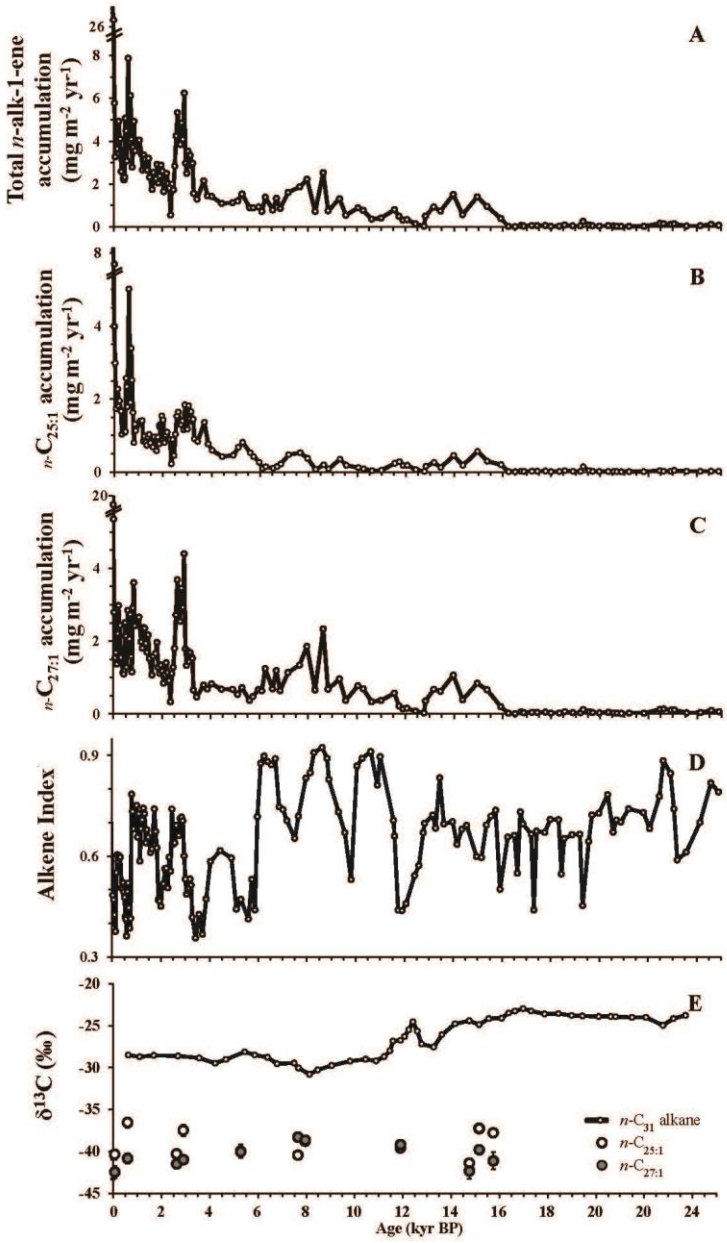

Figure 3: [A] Total (i.e., combined) accumulation of *n*-$C_{25:1}$ and *n*-$C_{27:1}$ alkenes (mg m^{-2} yr^{-1}). Accumulation of [B] *n*-$C_{25:1}$ and [C] *n*-$C_{27:1}$ alkene (mg m^{-2} yr^{-1}). [D] The Alkene Index, calculated as *n*-$C_{27:1}$/(*n*-$C_{25:1}$+*n*-$C_{27:1}$). [E] Carbon-isotopic ($\delta^{13}C$) values of *n*-$C_{25:1}$ (○) and *n*-$C_{27:1}$ (●) alkenes, compared with the $\delta^{13}C$ record of *n*-C_{31} alkanes (Sinninghe Damsté et al., 2011). Error bars show ± 1 standard deviation based on at least duplicate measurements. In many cases the error interval is smaller than the size of the symbol.

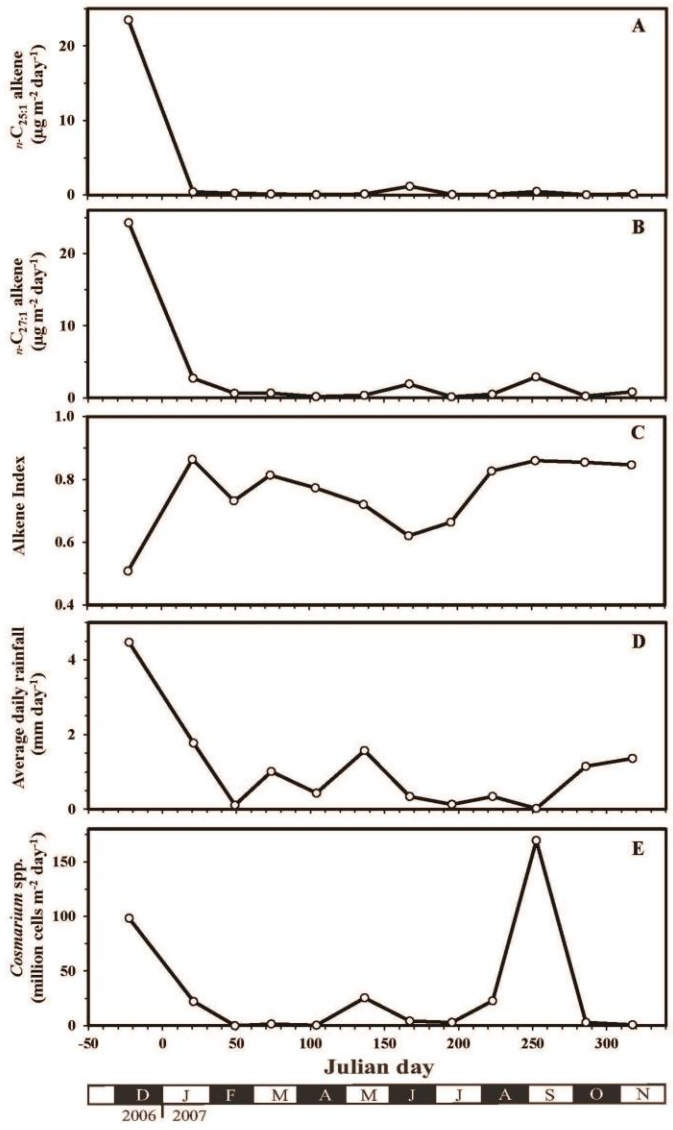

Figure 4: Monthly fluxes of alkenes and selected microalga in Lake Challa from November 2006 to December 2007, determined from materials settling in a sediment-trap deployed at 35 m water depth in the center of the lake, plotted on a Julian day time-scale. [A] *n*-$C_{25:1}$ and [B] *n*-$C_{27:1}$ alkene flux (µg m^{-2} day^{-1}). [C] The Alkene Index [*n*-$C_{27:1}$]/([*n*-$C_{25:1}$]+[*n*-$C_{27:1}$]). [D] Average rainfall (mm day^{-1}) during monthly periods of sediment-trap deployment in 2006/2007, from the Voi weather station 80 km to the east of Lake Challa (adapted from Sinninghe Damsté et al., 2009). [E] Monthly flux of the green alga *Cosmarium* spp., in million cells m^{-2} day^{-1}.

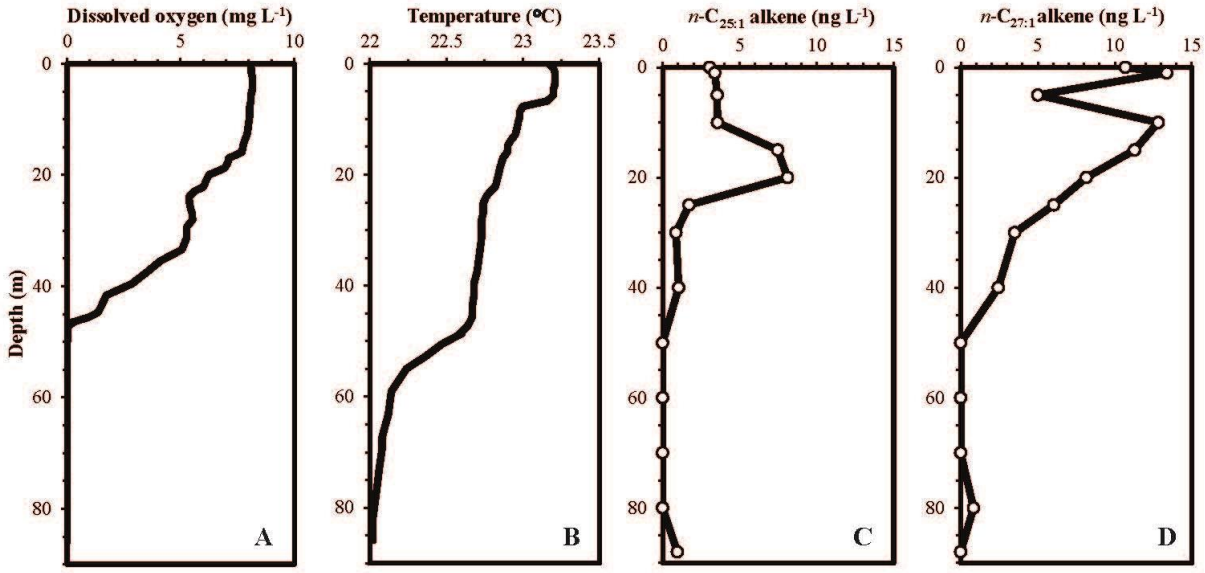

Figure 5: [A] Vertical distribution of dissolved oxygen (mg L^{-1}) and [B] temperature (°C) in the water column of Lake Challa, measured on 11-12 September 2006 (modified after Sinninghe Damsté et al., 2009). [C] *In-situ* concentrations of *n*-$C_{25:1}$ and [D] *n*-$C_{27:1}$ alkenes (ng L^{-1}) from SPM samples.

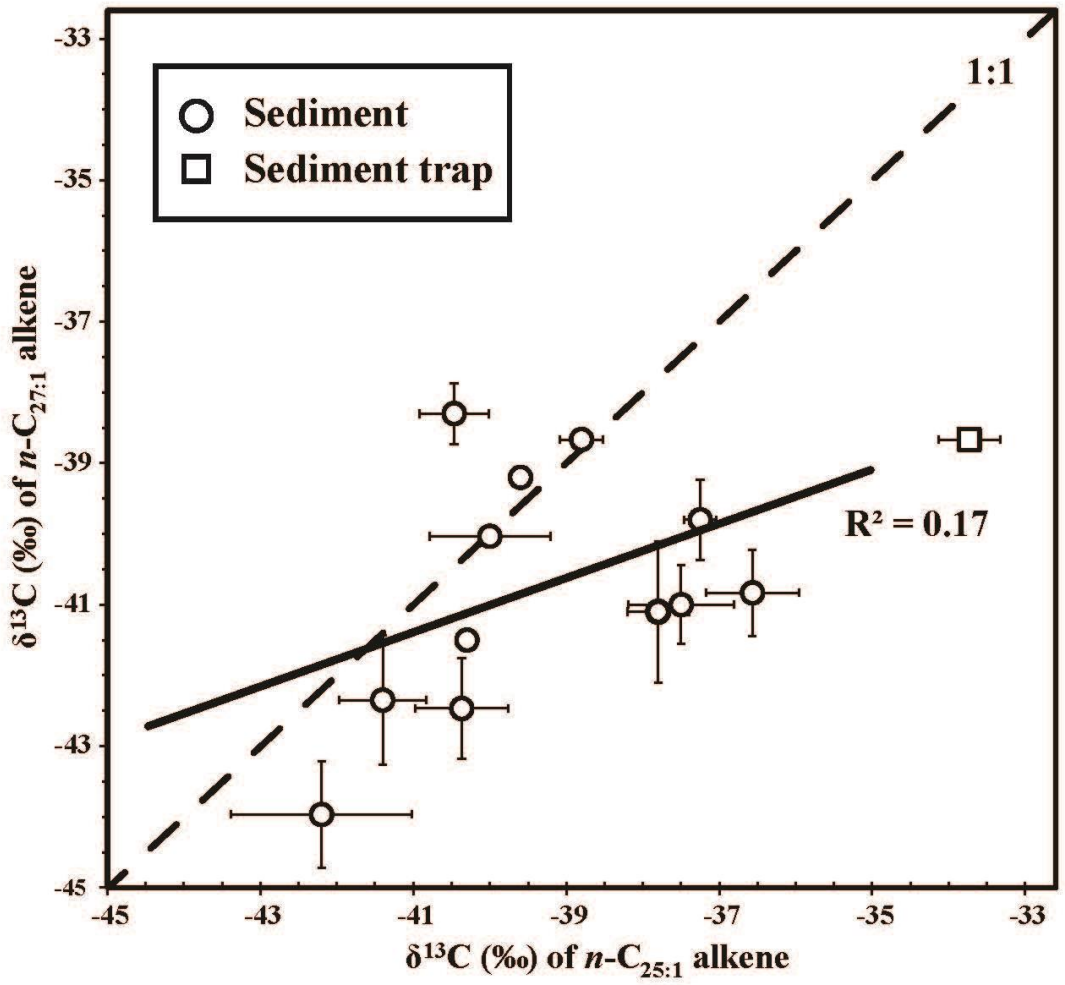

Figure 6: The stable carbon-isotopic composition ($\delta^{13}C$ in ‰ vs. VPDB) of *n*-$C_{25:1}$ versus *n*-$C_{27:1}$ alkenes of 12 sediment samples spanning the last 16 kyr (O) and one modern-day sediment-trap sample (□). Error bars indicate ± 1 standard deviation based on duplicate or triplicate measurements. In some cases the error intervals are smaller than the size of the symbol. The R^2 value of the trend line excludes the sediment-trap sample.

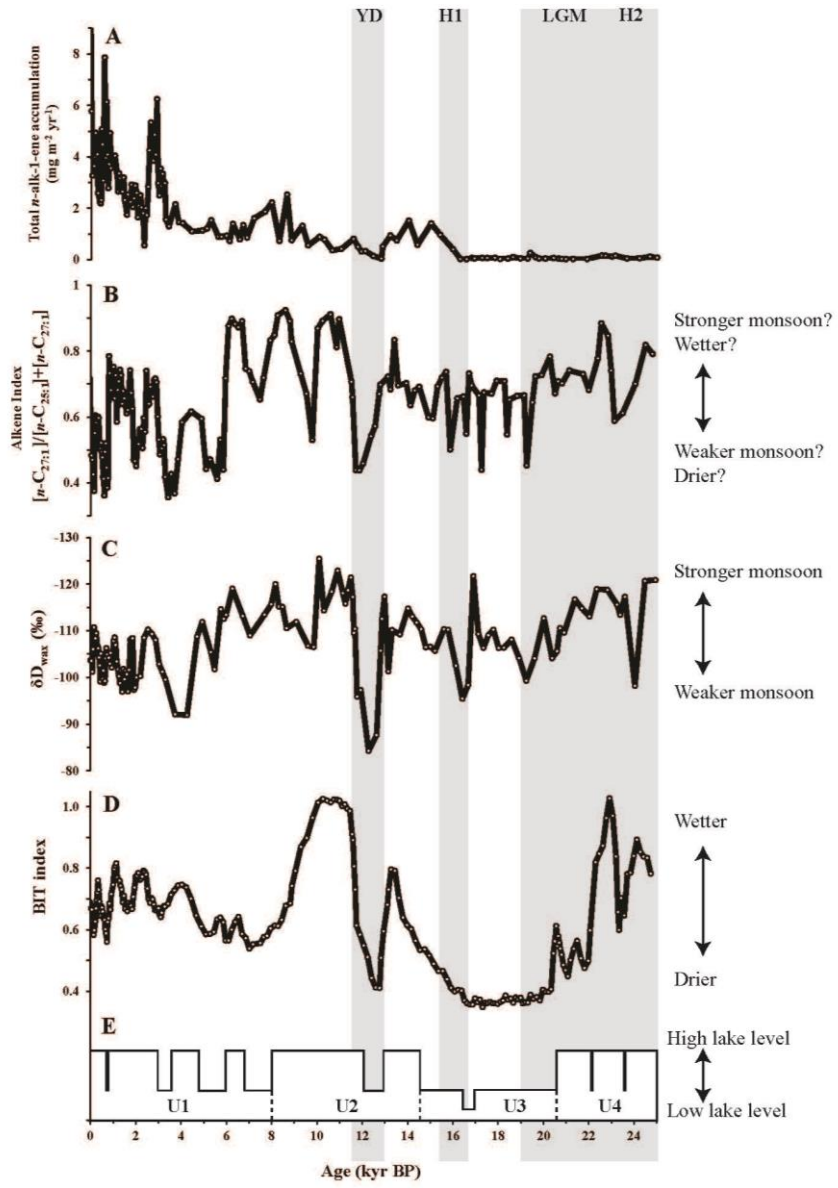

Figure 7: [A] Total (combined) accumulation of *n*-$C_{25:1}$ and *n*-$C_{27:1}$ alkenes (mg m^{-2} yr^{-1}). [B] The Alkene Index, defined as [*n*-$C_{27:1}$]/([*n*-$C_{25:1}$]+[*n*-$C_{27:1}$]). [C] The δD_{wax} record (‰ vs. VSMOW) on a reversed axis to highlight negative anomalies as episodes of inferred drought; adapted from Tierney et al. (2011). [D] The BIT-index, three-point moving average (Verschuren et al., 2009). [E] Lake Challa lake-level record derived from seismic-reflection data (Moernaut et al., 2010). Shaded areas represent Heinrich events H1 (16.8-15.4 kyr BP) and H2 (around 24 kyr BP), LGM (26.5-19 kyr BP) and YD (13-11.5 kyr BP).

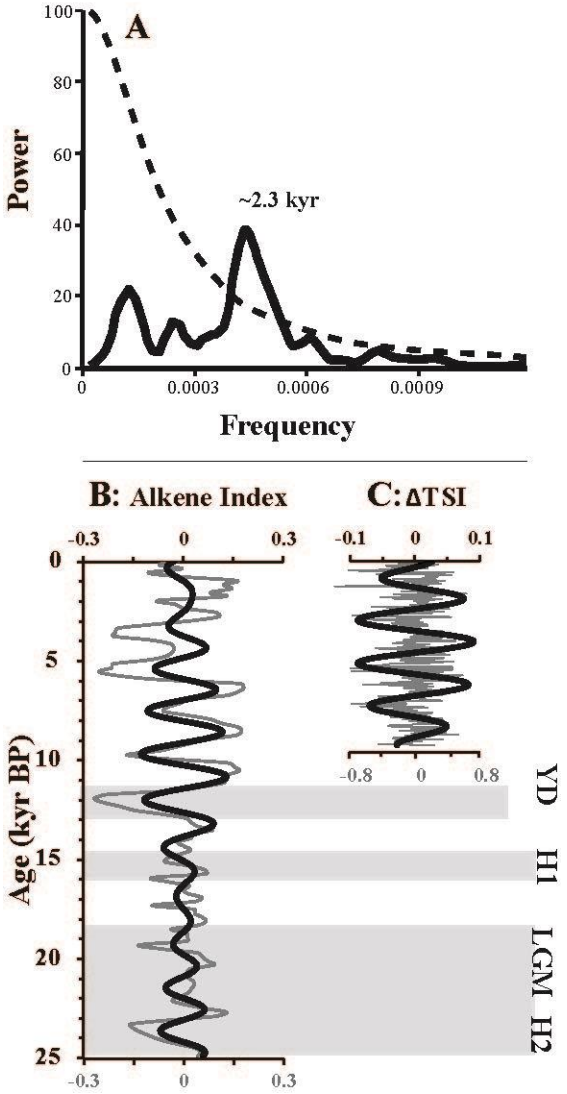

Figure 8: [A] REDFIT power spectrum estimation of the 25 kyr Alkene Index record from Lake Challa, revealing a main frequency of 2.3 kyr (p=0.0062). The dashed line represents the 99% significance level. Spectral analysis of resampled, detrended (grey lines) and filtered records (black lines) of [B] the Challa Alkene Index and [C] the difference of total solar irradiance (ΔTSI; in W m^{-2}; modified from Steinhilber et al., 2009). Shaded areas represent Heinrich events H1 (16.8-15.4 kyr BP) and H2 (around 24 kyr BP), LGM (26.5-19 kyr BP) and YD (13-11.5 kyr BP).

Table 1: Stable carbon-isotopic composition ($\delta^{13}C$, in ‰ vs. VPDB) of *n*-alk-1-enes and *n*-alkanes in Lake Challa sediments and sediment-trap.

Sediment Depth (cm)	**Age** (kyr BP)	**$C_{25:1}$ *n*-alkene** $\delta^{13}C$ in ‰ ±SD	**C_{25} *n*-alkane** $\delta^{13}C$ in ‰ ±SD	**$C_{27:1}$ *n*-alkene** $\delta^{13}C$ in ‰ ±SD	**C_{27} *n*-alkane** $\delta^{13}C$ in ‰ ±SD	**C_{31} *n*-alkane** $\delta^{13}C$ in ‰ ±SD
4-8	-0.001	-42.2 ±1.2	-35.4±0.1	-44.0 ±0.8	-35.4±0.2	-32.2±0.2
12.2-16	0.07	-40.4 ±0.6	NA	-42.5 ±0.7	NA	NA
80-84	0.6	-36.6 ±0.6	-33.6±0.4	-40.8 ±0.6	-31.9±0.2	-27.5±0.1
248-252	2.6	-40.3 ±0.1	-39.4±1.0	-41.5 ±0.1	-38.1±0.3	-31.0±1.3
268-272	2.9	-37.5 ±0.7	-33.5±0.1	-41.0 ±0.6	-33.7±0.2	-31.5±0.4
432-436	5.3	-40.0 ±0.8	-33.1±0.6	-40.0 ±0.2	-32.5±1.4	-30.5±0.6
648-652	7.7	-40.5 ±0.5	-38.4±a	-38.3 ±0.4	-34.8±0.3	-30.8±0.5
672-676	7.9	-38.8 ±0.3	NA	-38.7 ±0.2	-35.2±1.1	-31.2±0.3
984-988	11.9	-39.6 ±0.1	-37.2±0.7	-39.2 ±0.1	-33.5±0.2	-27.7±0.1
1140-1144	14.8	-41.4 ±0.6	-40.0±0.1	-42.4 ±0.9	-38.8±0.6	-29.7±0.3
1200-1204	15.2	-37.3 ±0.2	-35.7±a	-39.8 ±0.6	NA	-27.2±a
1236-1240	15.7	-37.8 ±0.4	-33.8±0.0	-41.1 ±1.0	-33.4±0.0	-24.2±0.1
Sediment trap	December 2006	-33.7 ±0.4	NA	-38.7 ±0.1	NA	NA

NA: Not available

a: No standard deviation: value based on one measurement